UCRL-JRNL-201456

Tilted Thick-Disk Accretion onto a Kerr Black Hole

P. C. Fragile, P. Anninos

December 15, 2003

Astrophysical Journal

Draft version December 10, 2003
Preprint typeset using LaTeX style emulateapj v. 16/07/00

TILTED THICK-DISK ACCRETION ONTO A KERR BLACK HOLE

P. Chris Fragile and Peter Anninos
University of California, Lawrence Livermore National Laboratory, Livermore, CA 94550
Draft version December 10, 2003

ABSTRACT

We present the first results from fully general relativistic numerical studies of thick-disk accretion onto a rapidly-rotating (Kerr) black hole with a spin axis that is tilted (not aligned) with the angular momentum vector of the disk. We initialize the problem with the solution for an aligned, constant angular momentum, accreting thick disk around a black hole with spin $a/M = J/M^2 = +0.9$ (prograde disk). The black hole is then instantaneously tilted, through a change in the metric, by an angle β_0. In this Letter we report results with $\beta_0 = 0$, 15, and 30°. The disk is allowed to respond to the Lense-Thirring precession of the tilted black hole. We find that the disk settles into a quasi-static, twisted, warped configuration with Lense-Thirring precession dominating out to a radius analogous to the Bardeen-Petterson transition in tilted Keplerian disks.

Subject headings: accretion, accretion disks — black hole physics — hydrodynamics — methods: numerical — relativity

1. INTRODUCTION

A common simplification in the study of black hole accretion is the assumption of axisymmetry. For analytic work this greatly simplifies the problem, while still allowing one to gain useful insights. For numerical work, this assumption has historically been necessitated by limitations in computing resources, which have only been overcome within the last decade. For a rotating black hole, this implies a perfect alignment (or anti-alignment) between the angular momenta of the black hole and the accreting gas. However, perfectly aligned accretion seems unlikely in most black hole systems (see Fragile et al. (2001) for a review of the arguments).

If an accretion disk is instead misaligned or tilted, it will be subject to differential Lense-Thirring precession. This precession results in a gravitomagnetic torque that tends to twist and warp the disk. In this Letter we present results of hydrodynamic simulations of tilted, inviscid, thick accretion disks. This work represents the first three-dimensional, fully relativistic simulations of tilted black-hole accretion flows.

2. INVISCID ACCRETING THICK DISKS

Inviscid, geometrically thick disks (often referred to as black hole tori) have been shown analytically (Fishbone & Moncrief 1976; Abramowicz et al. 1978) and numerically (Wilson 1972; Hawley et al. 1984; Hawley 1991) to be robust solutions in the limit that self-gravity, radiation, and viscosity are all negligible. As such, their applicability is limited to regions close to the black hole where the dynamical timescale may be short compared to viscous and radiative timescales. Further out from the black hole, such a disk may transition into a thin, Keplerian disk (e.g. Hawley & Balbus 2002).

In thick disks, the gas flows in an effective (gravitational plus centrifugal) potential. A critical feature of this potential in relativity is the presence of a sharp cusp at the inner edge of the accretion disk. This cusp is similar to the L_1 Lagrange point in a close binary system: mass transfer is driven by pressure-gradient forces and the accreted gas falls from the disk toward the black hole with no dissipation of angular momentum. Thus viscosity is not required for accretion in such a configuration.

The analytic solution for the structure of a thick disk has been worked out for both non-rotating and rotating black holes in the limit of axisymmetry (Fishbone & Moncrief 1976; Abramowicz et al. 1978). However, no such solution has been worked out for more general non-axisymmetric flows. Furthermore, it is not clear that a steady-state solution would result. The nonlinear, time-dependent, multidimensional nature of this problem provides strong motivation to apply a numerical approach, which is the aim of this Letter.

3. BASIC EQUATIONS

3.1. *Hydrodynamic Equations in Kerr Geometry*

In this work, the system of equations for relativistic hydrodynamics (see Anninos & Fragile 2003) is evolved in a "tilted" Kerr-Schild polar coordinate system $(t, r, \vartheta, \varphi)$. This coordinate system is related to the usual (untilted) Kerr-Schild coordinates (t, r, θ, ϕ) through a simple rotation about the y-axis by an angle β_0, such that

$$\begin{pmatrix} \sin\vartheta\cos\varphi \\ \sin\vartheta\sin\varphi \\ \cos\vartheta \end{pmatrix} = \begin{pmatrix} \cos\beta_0 & 0 & -\sin\beta_0 \\ 0 & 1 & 0 \\ \sin\beta_0 & 0 & \cos\beta_0 \end{pmatrix} \begin{pmatrix} \sin\theta\cos\phi \\ \sin\theta\sin\phi \\ \cos\theta \end{pmatrix}. \tag{3-1}$$

For a Schwarzschild ($a = 0$) or an aligned Kerr black hole ($\beta_0 = n\pi$, where $n = 0, 1, 2, ...$), the $(t, r, \vartheta, \varphi)$ and (t, r, θ, ϕ) frames are equivalent.

The computational advantages of the "horizon-adapted" Kerr-Schild form of the Kerr metric are described in Papadopoulos & Font (1998) and Font et al. (1998). The primary advantage is that, unlike Boyer-Lindquist coordinates, there are no singularities in the metric terms at the event horizon. This is particularly important for numerical calculations as it allows one to place the grid boundaries inside the horizon, thus ensuring that they are causally disconnected from the rest of the flow, without suffering

numerical instabilities that singularities (physical or numerical) might seed.

3.2. *Constant Angular Momentum Thick Disk*

The theory of stationary, relativistic thick disks (or tori) of constant angular momentum is well-established and has been presented in great detail elsewhere (e.g. Kozlowski et al. 1978). For this reason, we present only an abbreviated discussion here.

Surfaces of constant pressure in the torus are determined from the relativistic analog of the Newtonian effective potential Φ,

$$\Phi - \Phi_{in} = -\int_0^P \frac{\mathrm{d}P}{\rho h} \ , \tag{3-2}$$

where P is the fluid pressure, ρ is the density, h is the relativistic enthalpy, and Φ_{in} is the potential at the boundary of the torus (where $P = 0$). For constant angular momentum l, the potential is simply $\Phi = \ln(-u_t)$, where u_t is the specific binding energy. Provided $l > l_{ms}$, where l_{ms} is the angular momentum of the marginally stable Keplerian orbit, the potential $\Phi(r, \theta)$ will have a saddle point Φ_{cusp} at $r = r_{cusp}$, $\theta = \pi/2$. We can define the parameter $\Delta\Phi = \Phi_{in} - \Phi_{cusp}$ as the potential barrier (energy gap) at the inner edge of the torus. If $\Delta\Phi < 0$, the torus lies entirely within its Roche lobe. Such a configuration is marginally stable with respect to local axisymmetric perturbations and unstable to low-order non-axisymmetric modes (Papaloizou & Pringle 1984). If $\Delta\Phi > 0$, the torus overflows its Roche lobe and accretion occurs through the cusp. This accretion generally suppresses the growth of instabilities in the torus (Hawley 1991).

4. NUMERICAL RESULTS

Our main purpose in this work is to examine the structure of tilted accreting thick disks orbiting around a Kerr black hole. In practice, we actually leave the disks aligned with the computational grid and tilt the black hole through a transformation of the metric. This approach gives slightly better angular momentum conservation, although we have tested problems with the disk tilted relative to the grid and found the additional numerical diffusion to be small. We carry out these simulations using Cosmos, a massively parallel, multidimensional, radiation-chemo-hydrodynamics code for both Newtonian and relativistic flows. The relativistic capabilities and tests of Cosmos are discussed in Anninos & Fragile (2003). The present work utilizes the zone-centered artificial viscosity hydrodynamics package in Cosmos.

The simulations are initialized with the analytic solution for an axisymmetric black hole torus with $l = 2.6088$ and $a = 0.9M$. The surface of the tori are set by $\Phi_{in} = -0.01$ ($\Delta\Phi = 0.03$). The simulations are carried out on a grid extending from $0.98r_{BH} \le r \le 80M$, $0 \le \vartheta \le \pi$, and $0 \le \varphi < 2\pi$, where $r_{BH} = 1.44M$ is the radius of the black hole horizon and M is the mass of the black hole. These limits ensure that the disk is initially contained entirely within the computational domain. In order to increase the resolution in the inner region of the disk, we replace the radial coordinate r with a logarithmic coordinate $\eta = 1 + \ln(r/r_{BH})$, corresponding to a radial grid spacing of $0.2M$ near the horizon located at $\eta = 1$. The grid is resolved with $48\times24\times48$ zones along the dimensions $\eta,\ \vartheta,\ \varphi$.

In the "background" regions not determined by the initial torus solution, we initialize the gas following the spherical Bondi accretion solution. We fix the parameters of this solution such that the rest mass present in the background is negligible ($\lesssim 10^{-2}$) compared to the mass in the torus. Similarly, the mass accretion from the background is generally small ($\lesssim 10^{-3}$) compared to the mass accretion from the disk. The outer radial boundary for these models is held fixed with the analytic solution for all evolved fields. The inner radial boundary uses simple flat (zero gradient) boundary conditions. Data are shared appropriately across angular boundaries.

After the torus and background are initialized, the black hole is tilted by an angle β_0. In this Letter, we present results for $\beta_0 = 0$, 15, and 30°. Each model is evolved to $t = 2000M = 43.5\tau_{orb}$, where $\tau_{orb} = 46M$ is the orbital period measured at the pressure maximum of the axisymmetric torus. By this time each model had achieved a quasi-steady state [i.e. the variations in measured disk quantities such as mass accretion rate, tilt, and twist are small ($< 10\%$) over dynamical timescales]. The top row in Figure 1 shows logarithmically-spaced isocontours of density in the $y = 0$ plane at $t = 2000M$ for each of the three models. The spin axis of the black hole lies in the plane of the figure and is tilted toward the left for $\beta_0 > 0$. The bottom row shows corresponding isosurface plots looking down the initial symmetry axis of the torus. Together, these plots give a qualitative feel for the noticeable warp and twist of the disk for $\beta_0 = 15$ and 30°.

To describe these results in more quantitative terms, we analyze the cumulative precession in the disk as a function of radius. We define the precession angle (twist) of the disk as

$$\gamma(r) = \arccos\left[\frac{\mathbf{J}_{BH} \times \mathbf{J}_{Disk}(r)}{|\mathbf{J}_{BH} \times \mathbf{J}_{Disk}(r)|} \cdot \hat{y}\right] \ , \tag{4-1}$$

where

$$(J_{BH})_i = \begin{pmatrix} -aM\sin\beta_0 \\ 0 \\ aM\cos\beta_0 \end{pmatrix} \tag{4-2}$$

is the angular momentum vector of the black hole and

$$(J_{Disk})_\rho = \frac{1}{2}\epsilon_{\mu\nu\sigma\rho}\frac{L^{\mu\nu}S^\sigma}{(-S^\alpha S_\alpha)^{1/2}} \tag{4-3}$$

is the angular momentum vector of the disk, where

$$L^{\mu\nu} = \int \left(x^\mu T^{\nu 0} - x^\nu T^{\mu 0}\right) \mathrm{d}^3x \ , \tag{4-4}$$

and $S^\sigma = \int T^{\sigma 0}\mathrm{d}^3x$. The equations for $L^{\mu\nu}$ and S^σ are integrated over concentric radial shells of the grid. Thus our resolution of $\gamma(r)$ is dictated by the resolution of the grid. The unit vector $\hat{y}$ in Equation (4-1) points along the axis about which the black hole is initially tilted. Thus, $\gamma(r) = 0°$ throughout the disk at $t = 0$. In order to capture twists larger than 180°, we also track the projection of $\mathbf{J}_{BH} \times \mathbf{J}_{Disk}(r)$ onto $\hat{x}$, allowing us to break the degeneracy in arccos.

Analogous to the Bardeen-Petterson effect in thin, Keplerian disks (Bardeen & Petterson 1975; Kumar & Pringle 1985; Scheuer & Feiler 1996), we expect the Lense-Thirring precession to dominate provided $\tau_{LT} \lesssim \tau_{acc}$,

where $\tau_{LT} = \Omega_{LT}^{-1} = r^3/(2aM)$ is the Lense-Thirring precession timescale and $\tau_{acc} = M_{disk}(r)/\dot{M}$ is the accretion timescale for the disk. We determine the accretion timescale numerically using the definitions

$$M_{disk}(\eta) \equiv \int_0^{2\pi} \int_0^{\pi} \int_1^{\eta} D \mathrm{d}\eta \mathrm{d}\vartheta \mathrm{d}\varphi \tag{4-5}$$

and

$$\dot{M} \equiv \int_0^{2\pi} \int_0^{\pi} DV^{\eta} \mathrm{d}\vartheta \mathrm{d}\varphi \ , \tag{4-6}$$

where D is the generalized fluid density and V^{η} is the radial transport velocity in logarithmic coordinates. The accretion rate $\dot{M}$ is calculated at the black hole horizon. Figure 2 shows the radial dependence of τ_{LT} and τ_{acc} for $\beta_0 = 15$ and $30°$. Since $\tau_{LT} < \tau_{acc}$ for $\eta \lesssim 3$ ($r \lesssim 11M$), this is the region of the disk over which we expect Lense-Thirring precession to be important. Gas accreting through the disk should be largely unaffected until it passes through this radius, consistent with our results as shown in Figure 3, which gives the total precession angle as a function of the logarithmic radial coordinate for the two tilted disk models. Since $\dot{M}$ is nearly constant in both models for $t > 1000M$, the transition radius remains approximately stationary. Furthermore, the total precession observed at a given radius is relatively unchanging, since the accreting gas only has a limited amount of time to precess, set by the accretion timescale at the transition radius.

5. DISCUSSION AND SUMMARY

We have performed the first fully relativistic numerical study of "tilted" accretion disks around Kerr black holes. Such disks are subject to differential Lense-Thirring precession, resulting in a gravitomagnetic torque that tends to twist and warp the disk. As we show in this work, this precession dominates provided $\tau_{LT} \lesssim \tau_{acc}$. For the thick disks considered in this work, this effect is important out to relatively modest distances of $r \sim 10M$. However, these disks accrete on timescales short compared to other disk models, particularly thin, Keplerian disks. A plot of a typical accretion timescale for a Keplerian disk is included in Figure 2, showing that the Lense-Thirring precession in such a disk can be important out to very large distances ($r \sim 100M$). In future work, we plan to extend our results by considering larger disks with longer accretion timescales.

We also plan to extend this work by considering disks with efficient angular momentum transport (i.e. viscous or MHD disks). There, the dissipation of angular momentum may allow the inner region of the disk to relax into the rotation plane of the black hole, while the outer region remains close to its original tilted alignment - the Bardeen-Petterson effect (Bardeen & Petterson 1975; Kumar & Pringle 1985; Scheuer & Feiler 1996). This realignment is seen to some extent in the inviscid disks considered here (e.g. the third column of Figure 1), although it is expected to be more efficient in viscous disks, resulting in a sharper transition. This effect may be important in explaining a variety of phenomena observed in black-hole systems. First, the orbital frequency of the gas in the transition region between the tilted and untilted disks creates a characteristic frequency which may be important in explaining certain variability properties, such as quasi-periodic oscillations (Fragile et al. 2001). The Bardeen-Petterson effect could also have important implications for the directions in which jets might emanate from accreting, spinning black holes. If the region of the accretion disk closest to the black hole is responsible for determining the direction of jet collimation, this effect may explain the poor correlation between the orientation of jets from low-luminosity AGN and the disk plane of the host spiral galaxies (Kinney et al. 2000; Schmitt et al. 2002). This effect may also explain the apparent tilt of galactic X-ray binaries such as GRO J1655-40 (Fragile et al. 2001) and SAX J1819-2525 (Maccarone 2002).

This work was performed under the auspices of the U.S. Department of Energy by University of California, Lawrence Livermore National Laboratory under Contract W-7405-Eng-48.

REFERENCES

Abramowicz, M., Jaroszynski, M., & Sikora, M. 1978, A&A, 63, 221
Anninos, P., & Fragile, P. C. 2003, ApJS, 144, 243
Bardeen, J. M., & Petterson, J. A. 1975, ApJ, 195, L65
Fishbone, L. G., & Moncrief, V. 1976, ApJ, 207, 962
Font, J. A., Ibáñez, J. M. ., & Papadopoulos, P. 1998, ApJ, 507, L67
Fragile, P. C., Mathews, G. J., & Wilson, J. R. 2001, ApJ, 553, 955
Hawley, J. F. 1991, ApJ, 381, 496
Hawley, J. F., & Balbus, S. A. 2002, ApJ, 573, 738
Hawley, J. F., Smarr, L. L., & Wilson, J. R. 1984, ApJS, 55, 211
Kinney, A. L., Schmitt, H. R., Clarke, C. J., Pringle, J. E., Ulvestad, J. S., & Antonucci, R. R. J. 2000, ApJ, 537, 152
Kozlowski, M., Jaroszynski, M., & Abramowicz, M. A. 1978, A&A, 63, 209
Kumar, S., & Pringle, J. E. 1985, MNRAS, 213, 435
Maccarone, T. J. 2002, MNRAS, 336, 1371
Papadopoulos, P., & Font, J. A. 1998, Phys. Rev. D, 58, 24005
Papaloizou, J. C. B., & Pringle, J. E. 1984, MNRAS, 208, 721
Scheuer, P. A. G., & Feiler, R. 1996, MNRAS, 282, 291
Schmitt, H. R., Pringle, J. E., Clarke, C. J., & Kinney, A. L. 2002, ApJ, 575, 150
Wilson, J. R. 1972, ApJ, 173, 431

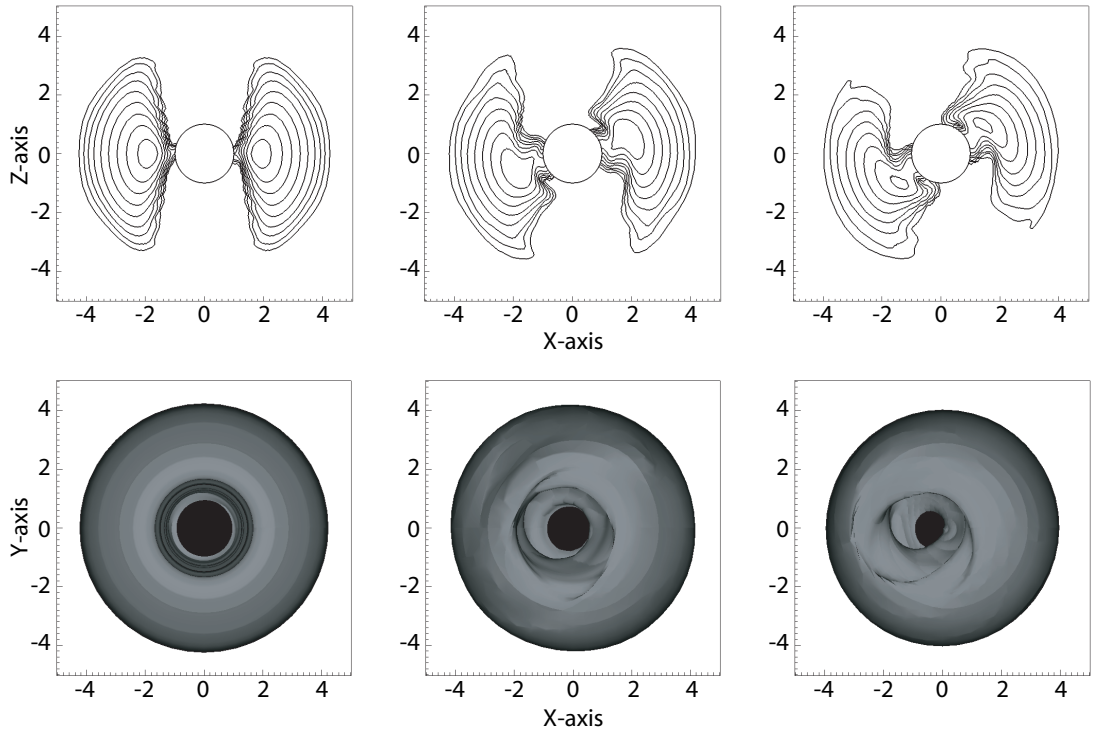

FIG. 1.— Logarithmically-spaced isocontours of density in the $y = 0$ plane (*top row*) and density isosurface plot looking down the initial symmetry axis of the torus (*bottom row*) for $\beta_0 = 0°$ (*left column*), $\beta_0 = 15°$ (*middle column*), and $\beta_0 = 30°$ (*right column*). Each panel is taken at $t = 2000M = 44\tau_{orb}$.

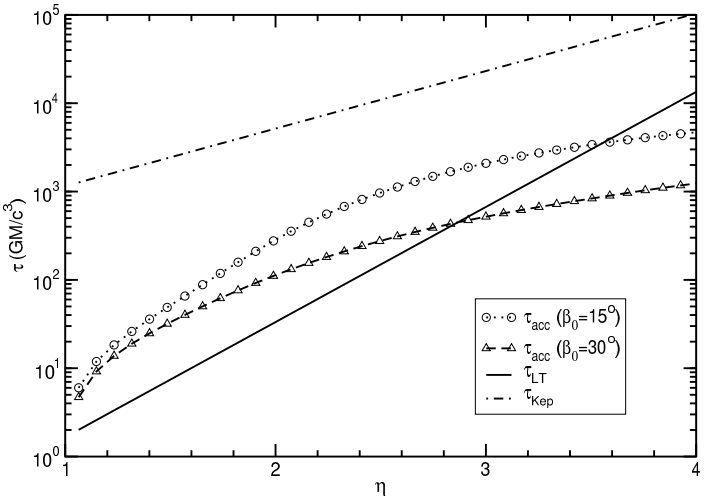

FIG. 2.— Plot of the accretion ($\tau_{mboxacc}$) and Lense-Thirring (τ_{mboxLT}) timescales as a function of the logarithmic radial coordinate η. Lense-Thirring precession is expected to be important provided $\tau_{LT} \lesssim \tau_{acc}$. The accretion timescales for $\beta_0 = 15$ and $30°$ correspond to $t = 2000M$ in the numerical simulations. Importantly, though, there is little variability in these curves for $t \gtrsim 1000M$. The accretion timescale for a thin Keplerian disk ($\tau_{mboxKep}$) is included for comparison.

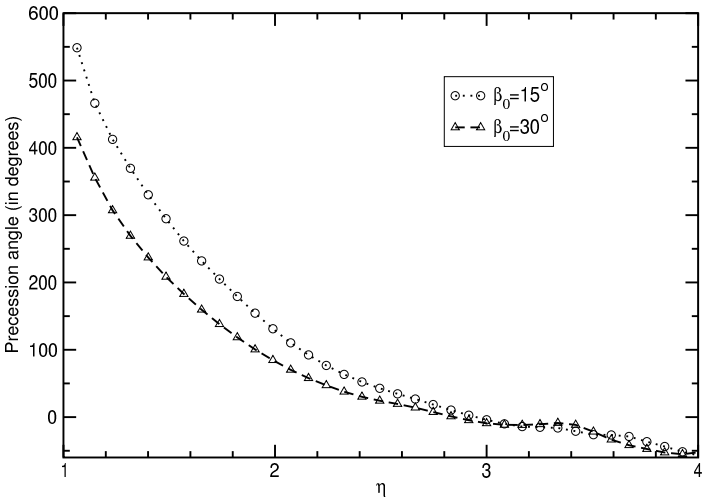

FIG. 3.— Plot of the total precession angle (γ) in degrees as a function of the logarithmic radial coordinate η for $\beta_0 = 15$ and 30° at $t = 2000M$. Importantly, there is little variability in these curves for $t \gtrsim 1000M$. Initially, $\gamma = 0^\circ$ throughout both disks.